



XXVIIIth International Conference on Ultrarelativistic Nucleus-Nucleus Collisions
(Quark Matter 2019)

Quenching of heavy and light flavour jets: experimental overview

Barbara Trzeciak

*Faculty of Nuclear Sciences and Physical Engineering
Czech Technical University in Prague
Brehova 7, 115 19 Prague, Czech Republic*

Abstract

In these proceedings, recent experimental results on jet quenching are discussed, focusing on measurements shown at the Quark Matter 2019 conference.

Keywords: heavy-ion collisions, jets, quenching, heavy-flavour, LHC, RHIC

1. Introduction

In the ultrarelativistic high-energy nuclear collisions, partons originating from the initial hard scatterings serve as probes of the structure of the medium created in the collisions. While traversing the hot and dense medium (QGP), the hard-scattered partons interact with the medium and lose part of their energy. It leads to an effect known as the *jet quenching*. The details of the parton-medium interactions and the energy loss mechanism are however still not fully understood. The thermodynamical and transport properties of the QGP, such as the medium transport coefficient \hat{q} , can be inferred from a model-to-data comparison.

Experimentally, the jet quenching can be studied via a modification of the high- p_T particle production or of fully reconstructed jets that are defined as collimated sprays of hadrons with a given resolution parameter R , most commonly reconstructed using the anti- k_T algorithm [1]. One can access the expected flavour dependence of the quenching for example by tagging jets with photons (thus increasing quark-seeded jet contribution) or with heavy-flavour hadrons. In central AA collisions, following has been observed: (i) a suppression of high- p_T charged hadrons, similar for different collision energies both at RHIC and LHC [2] (ii) no evidence of a flavour dependence at high $p_T > 10$ GeV/ c for charm [3] and > 20 GeV/ c for beauty [4], (iii) a strong suppression of the fully reconstructed jets up to p_T of a TeV [5].

In these proceedings, the recent experimental results on heavy- and light-jet quenching are discussed, focusing on a selection of measurements shown at this conference. The observables, related to the jet substructure, are excluded as they are a subject of a separate contribution.

2. Nuclear Modification Factor

The nuclear modification factor, R_{AA} , quantifies the deviation of inclusive spectra from the baseline, and is defined as:

$$R_{AA} = \frac{\frac{1}{N_{\text{event}}} dN^{AA}/dp_T d\eta}{\langle T_{AA} \rangle d\sigma^{pp}/dp_T d\eta}, \quad (1)$$

where N^{AA} is the yield in AA collisions, σ^{pp} is the proton-proton baseline cross section, and the T_{AA} is the nuclear overlap function.

2.1. R scan

Studying jets with different resolution parameters R gives an insight into the interplay of the suppression and recovery of the quenched energy. Systematic analyses of the jet nuclear modification factor as a function of the jet p_T and R provide additional constraints on the jet quenching models, and are complementary to jet substructure studies.

Figure 1(a) presents jet R_{AA} normalised to R_{AA} ($R = 0.2$), for several R parameter values between 0.2 and 1 measured by the CMS experiment, for $p_{T,\text{jet}} > 300$ GeV/c in 0–10% central Pb–Pb collisions at $\sqrt{s_{NN}} = 5.02$ TeV [6]. At high $p_{T,\text{jet}}$, the data show a mild increase of the $R_{AA}^R/R_{AA}^{R=0.2}$ ratio as a function of the jet R . The ALICE collaboration performed R_{AA} measurements at a lower jet p_T ranges, namely below 200 GeV/c down to $p_{T,\text{jet}}$ of 40–60 GeV/c, for the R parameter values of 0.2 and 0.4 [7] and recently also for $R = 0.6$ [8]. A strong jet suppression with a very little R dependence was observed.

The experimental results were compared to various predictions of jet quenching theoretical models, event generators and analytical calculations [9, 10, 11, 12, 13, 14, 15, 16, 17]. In the case of models, the different treatment of how the quenched energy is radiated and dissipated in the medium and of the medium response can result in significantly different trends of the jet R_{AA} vs R , especially at large R . This shows that the *basic* R_{AA} observable when extracted vs R and $p_{T,\text{jet}}$ has a strong constrain power among different jet quenching models. And data covering wider $p_{T,\text{jet}}$ and R ranges, in different collision centrality intervals, would be of a great importance here.

The current experimental results are limited to rather high jet p_T and/or small R , in particular in the most central collisions. This is due to the large and fluctuating background of the underlying event of particles uncorrelated with the hard scattering. At low p_T and in central collisions stronger medium effects on the jet are however expected. One of a promising solutions to deal with the large background corrections at low jet p_T and large R is to utilize Machine Learning techniques [19], as was demonstrated by the ALICE experiment [8].

2.2. Semi-inclusive jet measurements

Another way of performing jet analysis at lower p_T and large R parameter is to measure semi-inclusive jets recoiling from high- p_T trigger hadrons. This approach minimises jet selection biases. In addition, the large uncorrelated background can be suppressed using data-driven techniques.

The ALICE collaboration measured the Δ_{recoil} observable, defined as a difference between two semi-inclusive recoil jet distributions:

$$\Delta_{\text{recoil}} = \frac{1}{N_{\text{trig}}} \frac{d^2 N_{\text{jet}}}{dp_{T,\text{jet}}^{\text{ch}} d\eta_{\text{jet}}} \Bigg|_{p_{T,\text{trig}} \in \text{TT}_{\text{Sig}}} - c_{\text{Ref}} \cdot \frac{1}{N_{\text{trig}}} \frac{d^2 N_{\text{jet}}}{dp_{T,\text{jet}}^{\text{ch}} d\eta_{\text{jet}}} \Bigg|_{p_{T,\text{trig}} \in \text{TT}_{\text{Ref}}} \quad (2)$$

for $R = 0.2, 0.4$ and 0.5 at $20 < p_{T,\text{jet}} < 100$ GeV/c [18]. Figure 1(b) shows $\Delta_{\text{recoil}}^{\text{PbPb}}/\Delta_{\text{recoil}}^{\text{pp}}$ in the most central Pb–Pb collisions at $\sqrt{s_{NN}} = 5.02$ TeV. The results for different R are consistent within the uncertainties with a hint of increasing suppression with increasing R values at p_T below 40 GeV/c.

In the STAR experiment at RHIC, per-trigger recoil jet yields, $Y(p_{T,\text{jet}})$, triggered with π^0 ($11 < E_T^{\text{trig}} < 15$ GeV/c) were studied for two R parameter values of 0.2 and 0.5 [20]. At $\sqrt{s_{NN}} = 200$ GeV, the $R = 0.2$ results show jet suppression in central Au–Au collisions, while at $R = 0.5$ an indication of the energy recovery is observed, $Y^{\text{AuAu}}/Y^{\text{pp}}$ consistent with unity within the uncertainties with Pythia8 predictions used as the baseline.

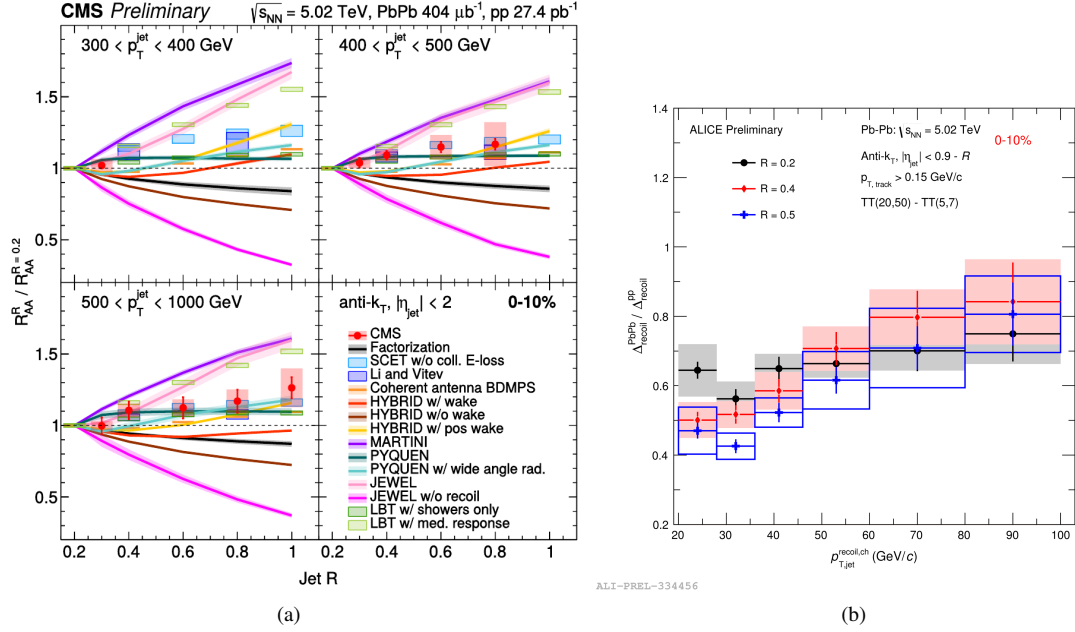


Fig. 1. (a) Jet R_{AA} ratio to $R_{AA}(R = 0.2)$ as a function of the R (in the range 0.3–1) for $p_{T,jet} > 300$ GeV/c, in 0–10% central Pb–Pb collisions at $\sqrt{s_{NN}} = 5.02$ TeV measured by the CMS experiment [6] (b) Pb–Pb/pp Δ_{recoil} ratio in most central Pb–Pb collisions at $\sqrt{s_{NN}} = 5.02$ TeV for $R = 0.2, 0.4$ and 0.5 measured by ALICE [18].

3. Path-length dependence of the energy loss

The path-length dependence of the parton in-medium energy loss can be probed by performing collision-system dependent measurements of the high- p_T hadron yield suppression. The LHC provided Pb ($\sqrt{s_{NN}} = 5.02$ TeV) and Xe ($\sqrt{s_{NN}} = 5.44$ TeV) ion beams. Taking into account the sizes of the two nuclei and under an assumption of quadratic (linear) dependence of the energy loss on the traversed path length, one expects a 31%(17%) reduction of the lost energy in head-on Xe–Xe collisions w.r.t. Pb–Pb [21]. Indeed, both CMS [21] and ALICE [22] reported R_{AA} in Xe–Xe to be larger compared to the Pb–Pb results in the same centrality classes. However, the data do not have enough constraining power among different models. An observable more sensitive to the path length dependence of the parton energy loss was proposed: $R_L^{XePb} = (1 - R_{AA}^{XeXe}) / (1 - R_{AA}^{PbPb})$, which may directly differentiate between different energy-loss mechanism from the experimental data [23]. The LHC data, together with the recent PHENIX measurements [24] of the R_{AA} in U–U, Au–Au and Cu–Cu collisions, also show that the high- p_T R_{AA} in different systems is compatible with each other at the same N_{part} value, which further proves dependence on the system size rather than the collision species.

STAR experiment introduced a technique called Jet Geometry Engineering (JGE) which aims to control the sampled parton path length in medium by biasing the selected jet sample [25, 26]. At RHIC energies, a requirement on a high momentum hadron trigger in a jet selects jets that are closer to the interaction region surface [27]. In addition, one can analyse di-jet configurations and by applying higher threshold on the momentum of the jet constituents select recoil jets with even longer path length in the medium. The main idea behind the JGE studies is to vary the constituent threshold and the jet radius in order to select di-jet samples with potentially different path lengths and so different energy losses. However, a theoretical input is essential to constrain the path length dependence of the partonic energy loss from these studies.

4. Redistribution of the quenched energy

It was observed that particles with low momenta associated with jets have a much broader angular distribution extending outside the jet [28, 29, 30, 31, 32] and their production is enhanced as compared to pp case [33, 34, 35, 36]. It suggests that the quenched energy is redistributed to large angles and in multiplicities of softer particles via a soft gluon emission. The ATLAS collaboration measured a distribution of charged particles at a distance r around the axis of jets with $R = 0.4$ [37]:

$$D(p_T, r) = \frac{1}{N_{\text{jet}}} \frac{1}{2\pi r dr} \frac{dn_{\text{ch}}(p_T, r)}{dp_T} \quad (3)$$

Modification of the distribution in Pb–Pb is quantified using a ratio to pp , $R_{D(p_T, r)}$, as shown in Fig. 2(a). An increasing enhancement of charged particles with $p_T < 4$ GeV/c as a function of the angular distance r from the jet axis is found, with the largest excess of particles within the jet cone. At the same time, particles with higher p_T are suppressed outside of the jet core. A small increase of the high- p_T particle yields in the core, up to $r = 0.05$, shall be also noted.

By measuring the away-side jet correlated with a high p_T π^0 , the PHENIX collaboration also observed an increase in low momentum particle production at wide angles, consistent with a wide angle gluon radiation. The analysis was performed via two-particle correlation of charged hadrons with high p_T neutral pions, integrating the charged-particle yield in the away-side region, Y . Figure 2(b) presents the PHENIX measurement of $I_{AA}(\Delta\phi) = Y^{AA}/Y^{pp}$ in central Au–Au collisions at $\sqrt{s_{NN}} = 200$ GeV for the trigger p_T in 4–7 GeV/c range and in $|\Delta\phi - \pi| < \pi/3$, and for different associated particle momentum range [24].

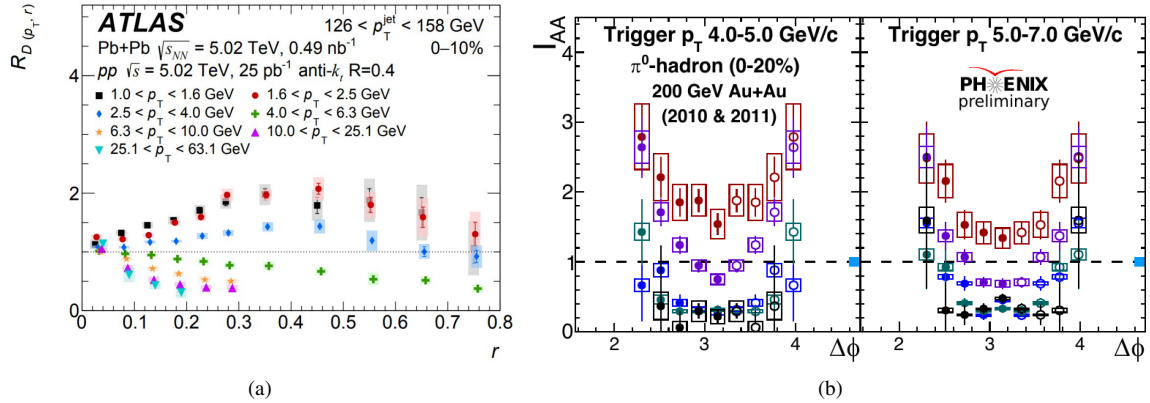


Fig. 2. (a) $R_{D(p_T, r)}$ distribution as a function of angular distance r for different ranges of charged-particle p_T , for $126 < p_{T, \text{jet}}$ measured by ATLAS in central Pb–Pb collisions at $\sqrt{s_{NN}} = 5.02$ TeV. (b) $I_{AA}(\Delta\phi) = Y^{AA}/Y^{pp}$ in central Au–Au collisions at $\sqrt{s_{NN}} = 200$ GeV measured by PHENIX [24], for two trigger p_T ranges: 4–5 and 5–7 GeV/c. Red, magenta, blue, green and black colours represent associate-particle p_T ranges of 0.5–1 GeV/c, 1–2 GeV/c, 2–3 GeV/c, 3–5 GeV/c, 5–7 GeV/c, respectively.

5. Boson tagged jets

Boson-tagged jets provide a controlled configuration of the initial hard scattering as photons or Z bosons do not interact strongly and are not modified by the medium. Moreover, at the LHC energies a high p_T jet sample is dominated by the quark-initiated jets.

Recent LHC results of photon-jet correlation can be found in the following references [38, 39, 40, 41]. Here, the latest ATLAS measurement of charged-particle per-Z yields opposite in azimuth to the Z boson [42] are presented. Thanks to a lower level of background compared to the γ -jet case, Z bosons can be studied in a lower p_T range. Figure 3(a) shows results of the charged-hadron p_T dependent Pb–Pb/ pp yield ratio, I_{AA} , for two Z boson p_T ranges of 30–60 and > 60 GeV/c. At high hadron p_T ($p_{T, \text{ch}}$) and $x_{hZ} = p_{T, \text{ch}}/p_{T, Z}$, the I_{AA} is significantly suppressed and the observed trends are qualitatively similar

to photon-tagged jet measurements. The Hybrid Strong/Weak Coupling model [43] and SCET_G [44, 45] (available for high x_{hZ}) reproduce the experimental outcome.

6. Flavour dependence of the energy loss

6.1. Gluon vs quark jets

Due to the colour factor, gluon-seeded jets are expected to be quenched more strongly while traversing the medium, as compared to quark jets. The charge of a jet is sensitive to the electric charge of the initiating parton, where charge is defined as a transverse-momentum weighted sum of the electric charges of the jet constituents q_i : $Q^\kappa = \frac{1}{(p_{T,jet})^\kappa} \sum_{i \in jet} q_i (p_T^i)^\kappa$, where κ controls sensitivity of the jet charge to low- and high- p_T constituents [46, 47]. It is predicted that even in heavy-ion collisions, the charge of different flavour jets remains distinct [45]. And under an assumption of a larger gluon than quark energy loss, jet charge is expected to increase from pp to central Pb–Pb collisions due to a larger fraction of quark jets remaining in the sample [48].

Figure 3(b) presents CMS results on a gluon-like jet fraction in pp and central Pb–Pb collisions at $\sqrt{s_{NN}} = 5.02$ TeV. Jets were reconstructed using anti- k_T algorithm with $R = 0.4$, $p_{T,jet} > 120$ GeV/ c and $|\eta| < 1.5$. The fraction of gluon jets was extracted by performing template fits to the jet charge distributions [49, 50]. The found gluon-like jet fraction in pp collisions is about 0.6 for minimum track $p_T > 1$ GeV/ c and $\kappa = 0.5$, consistent with PYTHIA predictions. Contrary to the expectations, no significant modification in the gluon- and quark-like jet fractions due to jet quenching in Pb–Pb collisions w.r.t. pp is observed for inclusive jets with $p_{T,jet} > 120$ GeV/ c . In addition, an increase of the width of the jet charge, as predicted for example by PYQUEN with radiative and collisional energy loss [51], is not seen in the data either.

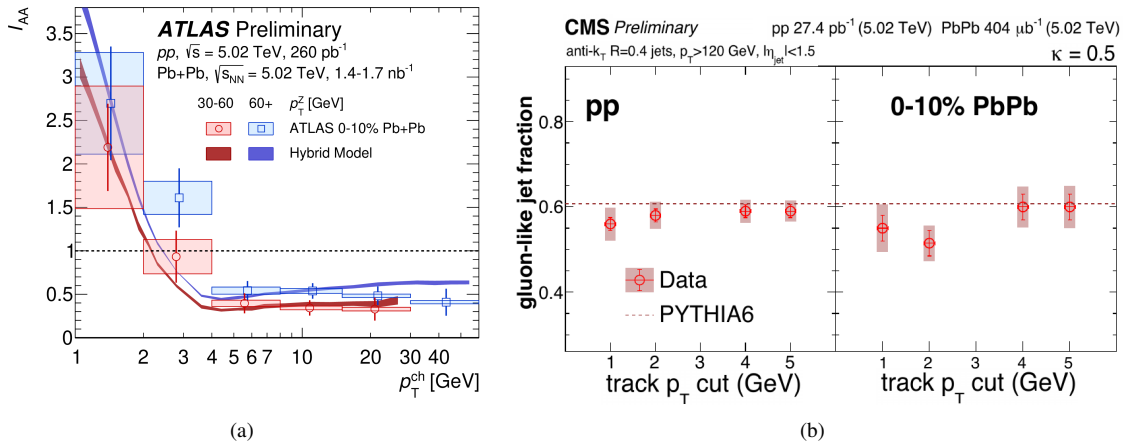


Fig. 3. (a) Ratio of charged-particle yield per Z boson between central Pb–Pb and pp collisions as a function of charged-hadron p_T , in two Z boson p_T ranges, compared to the Hybrid Model predictions [43]. (b) Gluon-like jet fractions in pp and 0–10% central Pb–Pb collisions as a function of a minimum track p_T , $p_{T,jet} > 120$ GeV/ c and $|\eta| < 1.5$.

6.2. Heavy-flavour jets

Studies of heavy-flavour jets provide information on the mass dependence of the parton energy loss. Due to the dead-cone effect heavier quarks are expected to lose less energy. But their measurements in heavy-ion collisions require high event rates and the heavy-flavour tagging is challenging due to the high background. The available experimental results are therefore scarce. Also, not many model predictions exist so far on the market. Within the current experimental uncertainties, the suppression of beauty-tagged jets as measured by CMS [52, 53] is consistent with the inclusive-jet one. ALICE experiment has capability to

study heavy-flavour hadrons at low p_T ranges. Studies of R_{AA} of jets tagged with D mesons were reported in $5 < p_{T,\text{jet}} < 20$ GeV/c in central Pb–Pb collisions [54]. Strong suppression at the same level as single D meson R_{AA} was observed. The suppression could not be directly compared to the inclusive jet result due to different covered $p_{T,\text{jet}}$ ranges.

Understanding the heavy-flavour jet production in pp collisions is important for interpretation of heavy-ion results. New measurements of D-meson- and b-tagged jets in pp collisions at $\sqrt{s} = 13$ and 5.02 TeV were presented [55] and compared to NLO pQCD calculations of POWHEG [56] coupled to the PYTHIA generator [57, 58]. The measured b-jet production cross-section agrees with the central values of the predictions while the charm-jet results are consistent with the upper edge of POWHEG at low $p_{T,\text{jet}}$ as also reported before in [59].

Furthermore, ALICE studied the fragmentation of heavy-flavour jets. The in-jet fragmentation data help to further constrain the heavy-flavour production and fragmentation in vacuum and the gluon fragmentation functions [60]. New measurements of the jet momentum fraction carried by the D meson or Λ_C baryon, $z_{\parallel}^{\text{ch}}$:

$$z_{\parallel}^{\text{ch}} = \frac{\vec{p}_{D(\Lambda_C)} \cdot \vec{p}_{\text{ch,jet}}}{\vec{p}_{\text{ch,jet}} \cdot \vec{p}_{\text{ch,jet}}}, \quad (4)$$

in pp collisions at $\sqrt{s} = 5$ and 13 TeV were presented [55]. In case of the D-tagged jets, a hint of softer fragmentation than the POWHEG+PYTHIA predicts was observed at low $p_{T,\text{jet}}$ (5–7 GeV/c), as can be seen in Fig. 4(a).

Similarly as in the case of the inclusive jet production in pA collisions [61, 62, 63, 64, 65], the heavy-flavour jet production is not modified w.r.t. pp collisions [55], which is consistent with an absence of a strong final state suppression. R_{pA} of heavy-flavour-electron-(HFE) and b-tagged jets is consistent with unity and with expectation from the POWHEG+PYTHIA with EPPS16 nPDFs [66], as presented in Fig. 4(b). The HFE-tagged jet production was analysed for different R values, $R = 0.3, 0.4$ and 0.6 , in both pp and p –Pb collisions. No dependence of the R_{pA} on R and no modification of the jet shape in p –Pb collisions, studied via $\sigma(R = 0.3)/\sigma(R = 0.6)$ ratio, was found [55, 67].

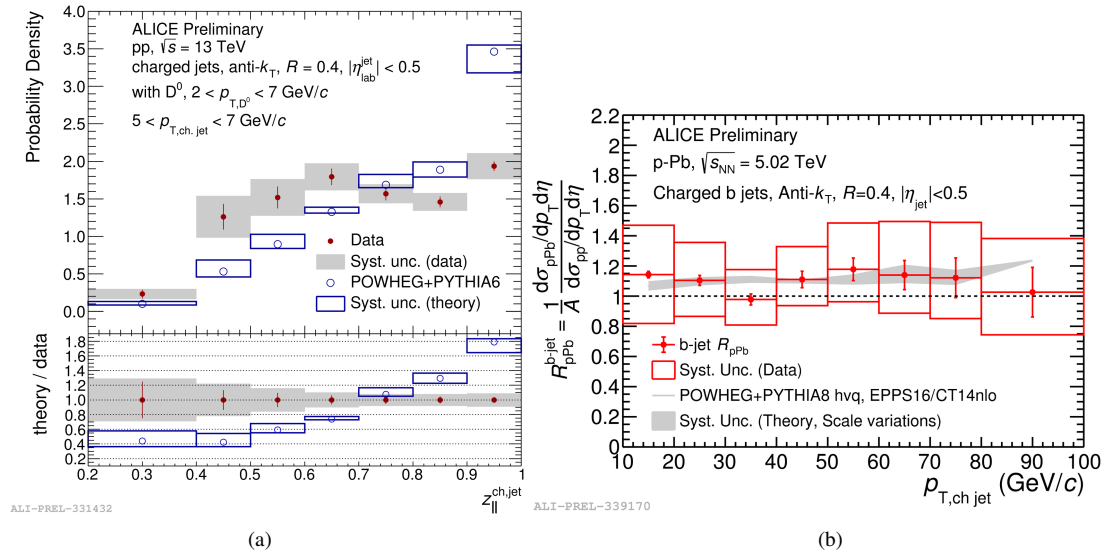


Fig. 4. (a): Probability density distribution of the jet momentum fraction, $z_{\parallel}^{\text{ch}}$, carried by D^0 meson in pp collisions at $\sqrt{s} = 13$ TeV for $5 < p_{T,\text{jet}} < 7$ GeV/c. (b) Nuclear modification factor, R_{pA} , of b-tagged jets in p –Pb collisions at $\sqrt{s_{NN}} = 5.02$ TeV compared to POWHEG+PYTHIA predictions with EPPS16 nPDF.

7. Summary

Thanks to the recent LHC and RHIC studies of the jet and high p_T hadron production in heavy-ion collisions, a more coherent picture of the parton in-medium energy loss starts to emerge. It has been observed that the lost energy is redistributed to large angles and soft particle multiplicities. Extensive R -dependent jet measurements were also performed. These new experimental results give better constraints on the jet quenching models, that should improve our understanding of the underlying parton energy loss mechanism and the medium response.

From the experimental side, it would be interesting to extend the current jet studies to large R in a wider $p_{T,\text{jet}}$ range, particularly in central collisions. Concerning the heavy-flavour tagged jets, the LHC Pb–Pb data from year 2018 have a potential to provide more precise results on charm and beauty jets, also in p_T intervals overlapping with the inclusive jet measurements. Moreover, it is important to perform complementary jet studies in heavy-ion collisions both at RHIC and LHC, varying in this way the medium temperature and probing different quark/gluon composition.

Acknowledgment

This work was supported by the grant CZ.02.1.01/0.0/0.0/16_013/001569 (Brookhaven National Laboratory - participation of the Czech Republic) of Ministry of Education, Youth and Sports of the Czech Republic.

References

- [1] M. Cacciari, G.P. Salam and G. Soyez, JHEP 04 (2008) 005, 0802.1188.
- [2] CMS, V. Khachatryan et al., JHEP 04 (2017) 039, 1611.01664.
- [3] ALICE, S. Acharya et al., JHEP 10 (2018) 174, 1804.09083.
- [4] CMS, A.M. Sirunyan et al., Phys. Rev. Lett. 123 (2019) 022001, 1810.11102.
- [5] ATLAS, M. Aaboud et al., Phys. Lett. B790 (2019) 108, 1805.05635.
- [6] CMS, CMS-PAS-HIN-18-014 (2019).
- [7] ALICE, S. Acharya et al., (2019), 1909.09718.
- [8] ALICE, R. Haake, 2019 European Physical Society Conference on High Energy Physics (EPS-HEP2019) Ghent, Belgium, July 10-17, 2019, 2019, 1909.01639.
- [9] CMS, V. Khachatryan et al., Eur. Phys. J. C76 (2016) 155, 1512.00815.
- [10] K.C. Zapp, Eur. Phys. J. C74 (2014) 2762, 1311.0048.
- [11] D. Pablos, Phys. Rev. Lett. 124 (2020) 052301, 1907.12301.
- [12] Y. He et al., Phys. Rev. C99 (2019) 054911, 1809.02525.
- [13] B. Schenke, C. Gale and S. Jeon, Phys. Rev. C80 (2009) 054913, 0909.2037.
- [14] J.W. Qiu et al., Phys. Rev. Lett. 122 (2019) 252301, 1903.01993.
- [15] R. Baier et al., Phys. Lett. B345 (1995) 277, hep-ph/9411409.
- [16] Y.T. Chien and I. Vitev, JHEP 05 (2016) 023, 1509.07257.
- [17] H.T. Li and I. Vitev, JHEP 07 (2019) 148, 1811.07905.
- [18] ALICE, Y. Mao, These proceedings .
- [19] R. Haake and C. Loizides, Phys. Rev. C99 (2019) 064904, 1810.06324.
- [20] STAR, N. Sahoo, Quark-Matter 2019 poster .
- [21] CMS, A.M. Sirunyan et al., JHEP 10 (2018) 138, 1809.00201.
- [22] ALICE, S. Acharya et al., Phys. Lett. B788 (2019) 166, 1805.04399.
- [23] M. Djordjevic et al., Phys. Rev. C99 (2019) 061902, 1805.04030.
- [24] PHENIX, A. Hodges, These proceedings .
- [25] STAR, L. Adamczyk et al., Phys. Rev. Lett. 119 (2017) 062301, 1609.03878.
- [26] STAR, R. Kunnawalkam Elayavalli, These proceedings .
- [27] T. Renk, Phys. Rev. C85 (2012) 064908, 1202.4579.
- [28] CMS, S. Chatrchyan et al., Phys. Rev. C84 (2011) 024906, 1102.1957.
- [29] CMS, V. Khachatryan et al., JHEP 01 (2016) 006, 1509.09029.
- [30] CMS, V. Khachatryan et al., JHEP 11 (2016) 055, 1609.02466.
- [31] CMS, A.M. Sirunyan et al., JHEP 05 (2018) 006, 1803.00042.
- [32] ALICE, S. Acharya et al., Phys. Lett. B796 (2019) 204, 1904.13118.
- [33] ATLAS, G. Aad et al., Phys. Lett. B739 (2014) 320, 1406.2979.
- [34] CMS, S. Chatrchyan et al., Phys. Rev. C90 (2014) 024908, 1406.0932.
- [35] ATLAS, M. Aaboud et al., Eur. Phys. J. C77 (2017) 379, 1702.00674.

- [36] ATLAS, M. Aaboud et al., Phys. Rev. C98 (2018) 024908, 1805.05424.
- [37] ATLAS, G. Aad et al., Phys. Rev. C100 (2019) 064901, 1908.05264.
- [38] CMS, A.M. Sirunyan et al., Phys. Lett. B785 (2018) 14, 1711.09738.
- [39] CMS, A.M. Sirunyan et al., Phys. Rev. Lett. 121 (2018) 242301, 1801.04895.
- [40] ATLAS, M. Aaboud et al., Phys. Lett. B789 (2019) 167, 1809.07280.
- [41] ATLAS, M. Aaboud et al., Phys. Rev. Lett. 123 (2019) 042001, 1902.10007.
- [42] ATLAS, D. Perepelitsa, These proceedings .
- [43] J. Casalderrey-Solana et al., JHEP 03 (2016) 053, 1508.00815.
- [44] Y.T. Chien et al., Phys. Rev. D93 (2016) 074030, 1509.02936.
- [45] H.T. Li and I. Vitev, (2019), 1908.06979.
- [46] ATLAS, G. Aad et al., Phys. Rev. D93 (2016) 052003, 1509.05190.
- [47] CMS, A.M. Sirunyan et al., JHEP 10 (2017) 131, 1706.05868.
- [48] S.Y. Chen, B.W. Zhang and E.K. Wang, Chin. Phys. C44 (2020) 024103, 1908.01518.
- [49] CMS, D. Hangal, These proceedings .
- [50] CMS, CMS-PAS-HIN-18-018 (2019).
- [51] I.P. Lokhtin, A.V. Belyaev and A.M. Snigirev, Eur. Phys. J. C71 (2011) 1650, 1103.1853.
- [52] CMS, S. Chatrchyan et al., Phys. Rev. Lett. 113 (2014) 132301, 1312.4198, [Erratum: Phys. Rev. Lett.115,no.2,029903(2015)].
- [53] CMS, A.M. Sirunyan et al., JHEP 03 (2018) 181, 1802.00707.
- [54] ALICE, B. Trzeciak, Nucl. Phys. A982 (2019) 579.
- [55] ALICE, J. Kvapil, These proceedings .
- [56] S. Frixione, P. Nason and C. Oleari, JHEP 11 (2007) 070, 0709.2092.
- [57] T. Sjostrand, S. Mrenna and P.Z. Skands, JHEP 05 (2006) 026, hep-ph/0603175.
- [58] T. Sjostrand, S. Mrenna and P.Z. Skands, Comput. Phys. Commun. 178 (2008) 852, 0710.3820.
- [59] ALICE, S. Acharya et al., JHEP 08 (2019) 133, 1905.02510.
- [60] D.P. Anderle et al., Phys. Rev. D96 (2017) 034028, 1706.09857.
- [61] PHENIX, A. Adare et al., Phys. Rev. Lett. 116 (2016) 122301, 1509.04657.
- [62] CMS, V. Khachatryan et al., Eur. Phys. J. C76 (2016) 372, 1601.02001.
- [63] CMS, S. Chatrchyan et al., Eur. Phys. J. C74 (2014) 2951, 1401.4433.
- [64] ATLAS, G. Aad et al., Phys. Lett. B748 (2015) 392, 1412.4092.
- [65] ALICE, J. Adam et al., Phys. Lett. B749 (2015) 68, 1503.00681.
- [66] K.J. Eskola et al., Eur. Phys. J. C77 (2017) 163, 1612.05741.
- [67] ALICE, S. Sakai, Quark-Matter 2019 poster .